

Atmospheric gravity waves observed in the nightglow following the 21 August 2017 total solar eclipse

I. Paulino¹, C.A.O.B. Figueiredo², F.S. Rodrigues⁴, R.A. Buriti¹,
C.M. Wrasse², A.R. Paulino³, D. Barros², H. Takahashi², I.S. Batista², A.F.
Medeiros¹, P. P. Batista², M.A. Abdu², E.R. de Paula², C.M. Denardini²,
L.M. Lima³, R.Y.C. Cueva⁵, J.J. Makela⁶

¹Unidade Acadêmica de Física, Universidade Federal de Campina Grande, Campina Grande, PB, Brazil

²Instituto Nacional de Pesquisas Espaciais, São José dos Campos, SP, Brazil

³Departamento de Física, Universidade Estadual da Paraíba, Campina Grande, PB, Brazil

⁴W. B. Hanson Center for Space Sciences, University of Texas at Dallas, Richardson, TX, USA

⁵Departamento de Física, Universidade Estadual do Maranhão, São Luís, MA, Brazil

⁶Department of Electrical and Computing Engineering, University of Illinois, Urbana-Champaign, IL, USA

Key Points:

- A multi-instrumented observational campaign was carried out in Brazil to study the effects of 21 August 2017 solar eclipse;
- Medium-scale gravity waves were observed in the airglow over the Northeastern Brazil;
- Analyses including reverse ray-tracing indicate the eclipse as the likely source for an observed medium-scale gravity wave.

Corresponding author: Igo Paulino, igo.paulino@df.ufcg.edu.br

Abstract

Nighttime airglow images observed at the low-latitude site of São João do Cariri (7.4°S, 36.5°W) showed the presence of a medium-scale atmospheric gravity wave (AGW) associated with the 21 August 2017 total solar eclipse. The AGW had a horizontal wavelength of $\sim 1,618$ km, observed period of ~ 152 min and propagation direction of $\sim 200^\circ$ clockwise from the north. The spectral characteristics of this wave are in good agreement with theoretical predictions for waves generated by eclipses. Additionally, the wave was reverse ray-traced and the results show its path crossing the Moon's shadow of the total solar eclipse in the tropical North Atlantic ocean at stratospheric altitudes. Investigation about potential driving sources for this wave indicate that the total solar eclipse as the most likely candidate. The optical measurements were part of an observational campaign carried out to detect the impact of the August 21 eclipse in the atmosphere at low latitudes.

Plain Language Summary

The Moon's shadow during a total solar eclipse introduces horizontal temperature gradients in the atmosphere and screens the ozone layer from solar heating. The shadow also travels supersonically producing instabilities that can generate the so-called atmospheric gravity wave (AGWs). AGWs associated with eclipses are expected to have periodic oscillations with periods ranging from just a few minutes to hours. Additionally, these AGWs can have horizontal wavelengths as large as thousand of kilometers. It is also possible to estimate the propagation path of the AGWs into the atmosphere by solving a system of equations that govern their propagation. This methodology is similar to that of tracing a ray of light that propagates in a varying environment. In the present work, an AGW in the northeast of Brazil was observed with spectral characteristics that indicate association with the 21 August 2017 total solar eclipse. In addition, the ray path matched the Moon's shadow in the stratosphere corroborating with the observational inferences. The AGW was observed by optical instruments during the nighttime, more than three hours after the end of the eclipse and over 2,000 km away from the Moon's shadow.

1 Introduction

Wind shear, convection and topography are often cited as the main sources of atmospheric gravity waves (AGWs) (e.g., Clemesha & Batista, 2008; Vadas et al., 2009; X. Liu et al., 2019, and references therein). However, events capable of creating disturbances in vertical pressure gradient and gravity balance might also induce the generation of AGWs. A solar eclipse produces a strong horizontal gradient of temperature and ionization flux in the atmosphere across the sunlit and covered areas. Additionally, the umbra moves supersonically creating instabilities at different levels of the atmosphere, which generate a wide spectrum of AGWs (e.g., Fritts & Luo, 1993, and references therein). More details on the generation of gravity waves and acoustic gravity waves during an eclipse can be found in Knížová and Mošna (2011), who used plain language to explain this process.

After a series of publications about the generation of gravity waves by solar eclipses in the beginning of the 1970s decade (Chimonas & Hines, 1970, 1971; Chimonas, 1974), several experiments were carried out to investigate the characteristics of these gravity waves in the neutral atmosphere and their manifestation as traveling ionospheric disturbances (TIDs) in the ionosphere. The early experiments included observation of the eclipse of 7 March 1970 solar eclipse over the central and east coast of North America, which showed only some agreement between observa-

tions and theoretical predictions (e.g., Davis & Da Rosa, 1970; Arendt, 1972; Lerfald et al., 1972; Sears, 1972).

Several other experiments followed up trying to reconcile observations and theories related to AGWs and TIDs induced by eclipses (e.g., Beer & May, 1972; Frost & Clark, 1973). For instance, the experiments performed on 30 June 1973 identified AGWs and TIDs that were likely associated with the total solar eclipse that was observed crossing central Africa (e.g., Schödel et al., 1973; Anderson & Keefer, 1975; Broche & Crochet, 1975; B. W. Jones & Bogart, 1975). On 23 October 1976, AGWs and TIDs were also observed in South Australia associated with the eclipse (e.g., Beer et al., 1976). A few years later, on 26 February 1979, an eclipse was observed over North America and Greenland and new studies on the ionospheric responses to eclipses were conducted (e.g., Narcisi et al., 1983).

During the 1980s, only two solar total eclipses crossed the continental areas, one on 16 February 1980 over Africa and Asia and another on 29 March 1987 over Africa. Again, AGWs and TIDs were observed during those events (e.g., Hanuise et al., 1982; Mohanakumar & Sankaranarayanan, 1982). In the 1990s, five eclipses were observed over inhabited areas (11 July 1991, 03 November 1994, 24 October 1995, 8-9 March 1997 and 11 August 1999). Unfortunately, only a few AGW/TID experiments were performed during those events (e.g., Altadill et al., 2001; Aplin & Harrison, 2003; T. B. Jones et al., 2004). In the past two decades at least ten total solar eclipses occurred (21 June 2001, 04 December 2002, 08 April 2005, 29 March 2006, 01 August 2008, 21-22 July 2009, 13-14 November 2012, 03 November 2013, 21 August 2017 and 02 July 2019) over continental areas which allowed important ground-based observation of AGWs and TIDs (e.g., Zerefos et al., 2007; Afraimovich et al., 2007; Chen et al., 2011; Paul et al., 2011; Amabayo et al., 2014; K. V. Kumar et al., 2016; S. Kumar et al., 2016; Paulino et al., 2018; Vargas, 2019).

From the observations, several aspects of AGWs and TIDs induced by eclipses were learned. For instance, it was found that bow waves, generated by the Moon's shadow traveling at a supersonic speed, could be detected in parameters of neutral atmosphere and ionosphere. It was also found that periodic AGWs/TIDs with periods ranging from a few up to tens of minutes and wavelength extending up to a thousand kilometers could be observed during eclipse events. It must be pointed out that the spectral characteristics of the observed AGWs/TIDs depend on the distance where they were measured to the umbra of the eclipse. Furthermore, the wind system and the dissipative processes impose a natural filtering system, which limits the observable spectrum of AGWs at different atmospheric levels.

The total solar eclipse on 21 August 2017 presented a major opportunity to advance the understanding of the characteristics of AGWs (e.g., Coster et al., 2017, and references therein) and other atmospheric phenomena associated with the eclipse. The path of the umbra crossed the continental United States (US) (e.g., McInerney et al., 2018), and allowed, perhaps, the most comprehensive set of experiments to be conducted to date.

In addition to the experiments in the US, a multi-instrumented campaign of observations was carried out in the Northeast region of Brazil. The experiment was performed to determine the effects of the 21 August 2017 eclipse in the upper atmosphere at low latitudes including the occurrences of AGWs. The geographical location of the instruments operated during the campaign allowed, for the first time, this type of nighttime observations in Brazil. Signatures of gravity waves induced by eclipses have, however, already been observed in the rotational temperature during the night of 29 March 2006 (Aushev et al., 2008).

In the present work, the main results of the observations made by an all-sky imager located at São João do Cariri (7.4° S, 36.5° W, dip angle: 11° S) are presented and discussed. The imager detected a medium-scale AGW just three hours after the end of eclipse, which occurred over the Atlantic ocean around 21:04 universal time (UT). The observed wave shows spectral characteristics and propagation direction that are compatible with their generation by an eclipses. Additionally, the potential propagation path of the AGW was derived using reverse ray-tracing and it was found that the position of the likely source is within the region of the umbra in the stratosphere. Finally, observations of horizontal wind made at the same site using a Fabry-Perot Interferometer also indicate signatures of large-scale gravity waves in the thermosphere associated with the eclipse (Harding et al., 2018), which reinforces that AGWs induced by the 21 August 2017 solar eclipse can be observed far away from its source.

2 Image Analysis and Results

Coordinated multi-instrumented observations of the upper atmosphere were made around the total solar eclipse of 21 August 2017 in the Northeast region of Brazil. The main objective of those observations was the detection of gravity waves and ionospheric disturbance associated with the eclipse. The network of instruments included: (a) three digisondes (e.g., Batista et al., 2017) located at São Luís (2.58° S, 44.2° W), Fortaleza (3.87° S, 38.41° W) and Cachoeira Paulista (22.67° S, 45.00° W); (b) one very high frequency (VHF) coherent backscatter radar (e.g., Rodrigues et al., 2013) at São Luís; (c) one meteor radar at Cachoeira Paulista (e.g., A. R. Paulino et al., 2012); (d) a network of fluxgate magnetometers distributed over the Brazilian territory (e.g., Denardini et al., 2018); (e) one Fabry-Perot interferometer at São João do Cariri (e.g., Makela et al., 2009) and (f) one all-sky airglow imager at São João do Cariri (e.g., I. Paulino et al., 2016). In this note, the investigation focused on the observations made by the all-sky imager. The main results of these observations were presented and discussed during the 42nd COSPAR Scientific Assembly (Paulino et al., 2018).

Images of the near-infrared OH and atomic Oxygen at 630.0 nm (OI6300) airglow emissions were collected during the night of 21 August 2017 every two minutes in order to properly monitor the AGW activity in the mesosphere and lower thermosphere region after the end of the eclipse over the northeast of Brazil. The nominal height of the peak for the OH is ~ 87 km and the emission is proportional to the concentration of Ozone and Hydrogen. Therefore, it reflects the variation in the minor constituents of the mesosphere and lower thermosphere (MLT). The nominal height of the OI6300 emission is ~ 250 km and the emission intensity is proportional to the concentration of O_2 , N_2 and electrons in the thermosphere, which reflects variation in the concentration of ionospheric plasma. Signatures of AGWs propagating southward and southwestward were identified in the OH images after 00:00 UT.

To estimate horizontal AGW parameters (e.g., observed period, wavelength and direction of propagation) in the images, two techniques were used: (1) The two-dimensional Fast Fourier Transform (FFT) and cross-correlation spectrum (Garcia et al., 1997) and (2) Analysis of keograms (e.g., Shiokawa et al., 2009). The first technique is often used to estimate parameters of small-scale gravity waves and the second one is better used to study medium-scale gravity waves (e.g., I. Paulino et al., 2011; Campos et al., 2016; Essien et al., 2018).

The observations were complemented by additional numerical analysis. Reverse ray-tracing analysis was carried out to estimate the propagation path and to identify potential sources for the observed waves. The ray-tracing methodology is de-

scribed in Vadas and Fritts (2009) and has already been used to investigate sources of AGWs in the equatorial region (e.g., Sivakandan et al., 2016, 2019). In summary, the ray path for AGWs propagating into the atmosphere is obtained solving the following set of equations:

$$\frac{dx_i}{dt} = V_i + \frac{\partial \omega_{Ir}}{\partial k_i} = V_i + c_{g_i} \quad (1)$$

and

$$\frac{dk_i}{dt} = -k_j \frac{\partial V_j}{\partial x_i} - \frac{\partial \omega_{Ir}}{\partial x_i} \quad (2)$$

where x_i and k_i are the position and wavenumber of the wave at a given time, V_i is the neutral wind velocity, ω_{Ir} is the intrinsic frequency and c_{g_i} is the group velocity. Repeated indices indicate summation, e.g., “ j ”. Temperature from the Naval Research Laboratory Mass Spectrometer Incoherent Scatter Radar 2000 (NRLMSIS-00, Picone et al., 2002) and winds from the Horizontal Wind Model 2014 (HWM-14, Drob et al., 2015) were used as input for the ray-tracing technique.

Analysis of the OH all-sky images show the occurrence of small- and medium-scale AGWs. The reverse ray-tracing results for small-scale AGWs (observed periods of ~ 10 min and horizontal wavelengths of ~ 30 km) showed that these waves reached tropospheric altitudes in the region near the observatory, i.e., only a few hundred of kilometers away. In addition to small-scale waves, two medium-scale gravity waves were identified, the first medium-scale AGW had a period of ~ 47 min, a horizontal wavelength of ~ 580 km and propagated to the southeast. The result from the ray-tracing indicated that the likely source was located over the ocean, to the northwest of the observatory. The second medium-scale AGW is going to be the focus of the present investigation. It had a period of ~ 150 min, a horizontal wavelength of $\sim 1,600$ km and propagated southwestward (azimuth of 200° from the North clockwise). Therefore, the propagation direction suggested a connection with the eclipse.

Figure 1 shows the keogram results for the all-sky images when a medium-scale AGW was observed. Panels A) and B) of Figure 1 show the East-West (E-W) and North-South (N-S) cuts of the images as a function of the time (keograms), respectively. From the keograms, amplitudes (A_m), horizontal wavelength (λ_H), observed period (τ), horizontal phase speed (c_H) and propagation direction (ϕ) are derived. These parameters are indicated in Panel C) which also shows the spectrum of fluctuations in the E-W direction. Panel D) shows the spectrum of fluctuations in the N-S direction and the uncertainty in the derived parameter values. Details about the derivation of these parameters of AGWs from keograms can be found in Appendix A of Figueiredo et al. (2018). One can see in Figure 1A) one crest on the central portion of the keogram, while Figure 1B) shows one crest in the beginning and one valley towards the end part of the keogram. Note that, besides the medium-scale structure, the keograms also show other small oscillations.

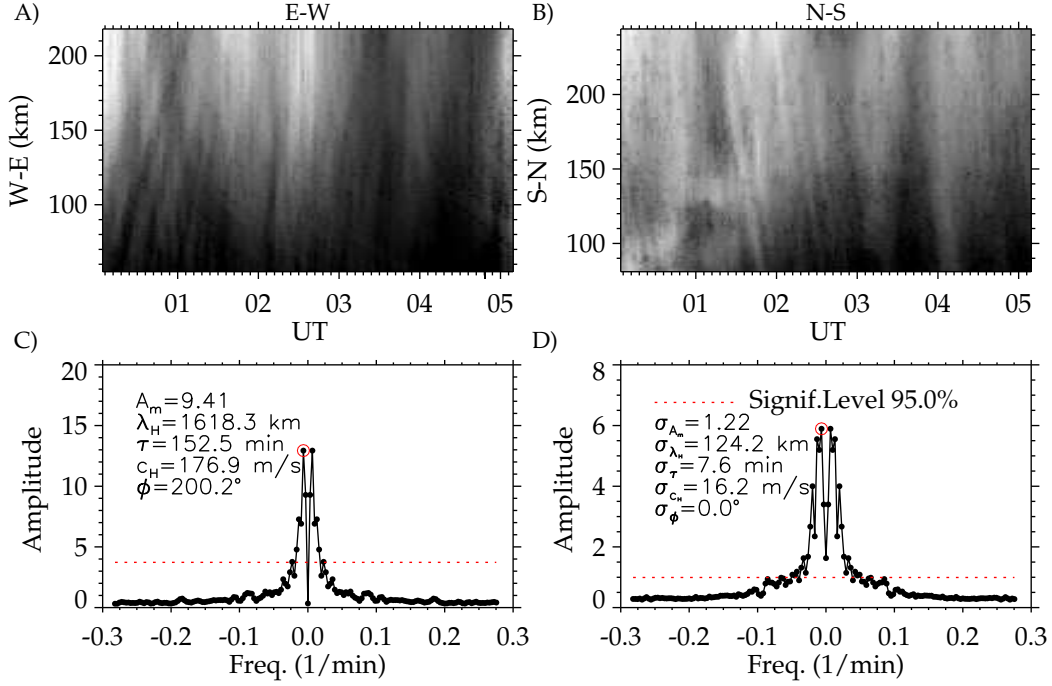


Figure 1. Keogram analysis for East-West (left side) and North-South (right side). Panels (A) and (B) show the keograms from the airglow images. Panels (C) and (D) show the amplitude of the main oscillations.

Figure 2 shows the path of the medium-scale AGW derived from the reverse ray-tracing assuming two distinct background wind patterns. The dashed red line represents the results for zero wind model. The solid green line represents the results for the HWM-14 winds. Comparison using zero wind and modeled wind gives an idea about the effect of the wind in changing the trajectory of the wave into the atmosphere. In the present case, only small differences were noted. Furthermore, the black heavy line shows the path of the Moon's shadow and the blue spots represent regions with cold clouds, which can indicate local instability. Cloud temperature information was obtained from Geostationary Operational Environmental Satellites (GOES) from the infrared images of the clouds. The occurrence of cold clouds has been used to identify convection and potential sources of small-scale AGWs (Dare-Idowu et al., 2020). The color bar on the top of Figure 2 shows the temperature scale in degrees Celsius. The blue spots in Figure 2 indicate the occurrence of convection near the end of the eclipse path, in the Amazon region and over the North tropical Atlantic ocean. Note that the ray-tracing results show that the path of the medium-scale AGW crossed the end of the eclipse and extended horizontally over 1000 km to the northeast direction.

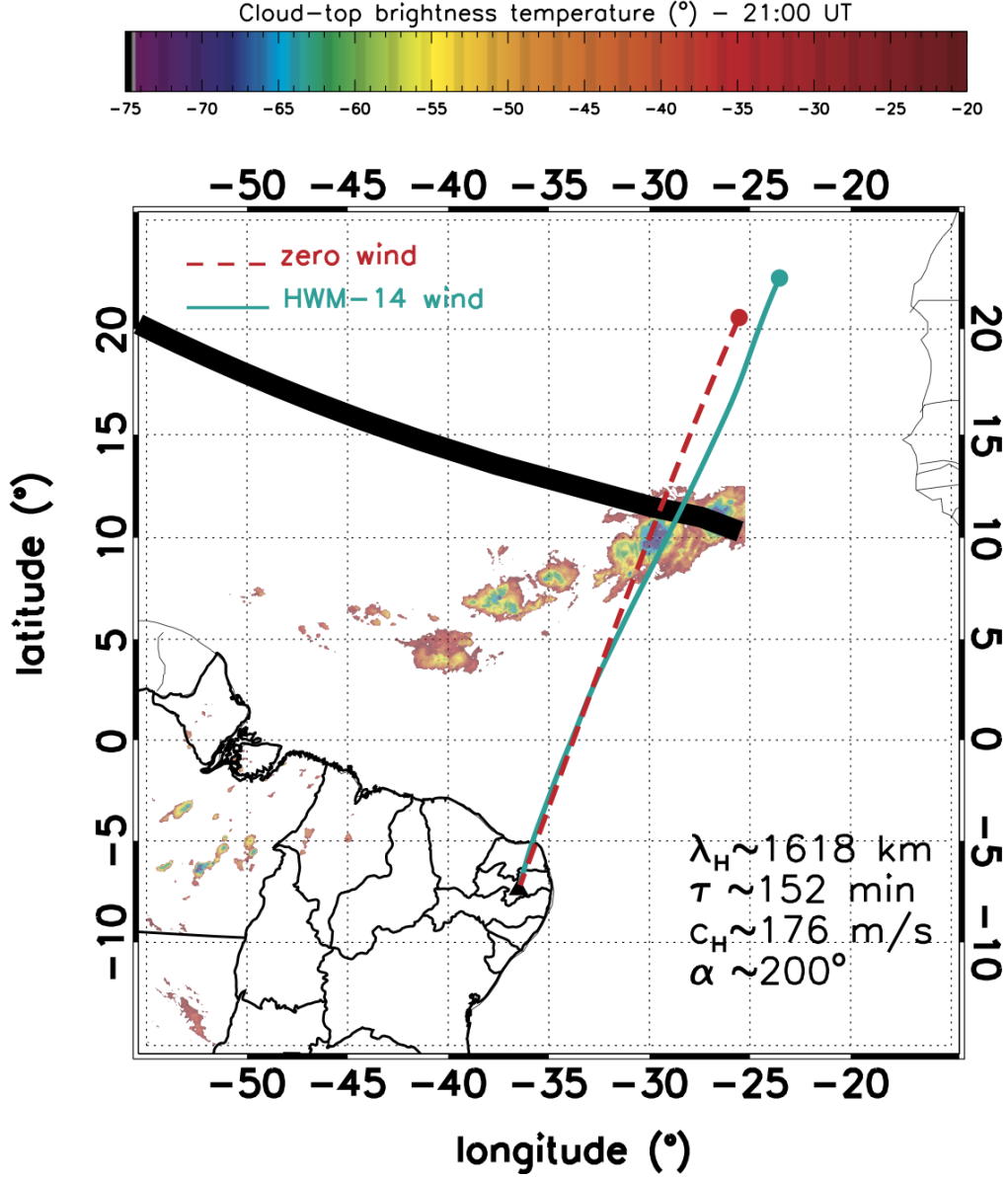


Figure 2. The ray path of the gravity wave on a geographical map. The red dashed line represents the ray path using zero wind condition and the solid green line represents the HWM-14 wind condition. The black heavy line represents the Moon's shadow. The rainbow spots represent clouds in which the estimated temperature is shown in the color bar on the top. Colder clouds are shown in violet and indicates deep convection and very high clouds.

Figure 3 shows the results for the temporal evolution of the gravity wave ray path into the atmosphere. Again, results for the HWM-14 wind model and for zero winds converge to similar paths. The horizontal black line represents the altitude where the ray path crossed the Moon's shadow, which is around 34.4 km altitude, i.e., in the stratospheric heights. These results show that this medium-scale gravity wave likely had its sources in the north tropical Atlantic ocean.

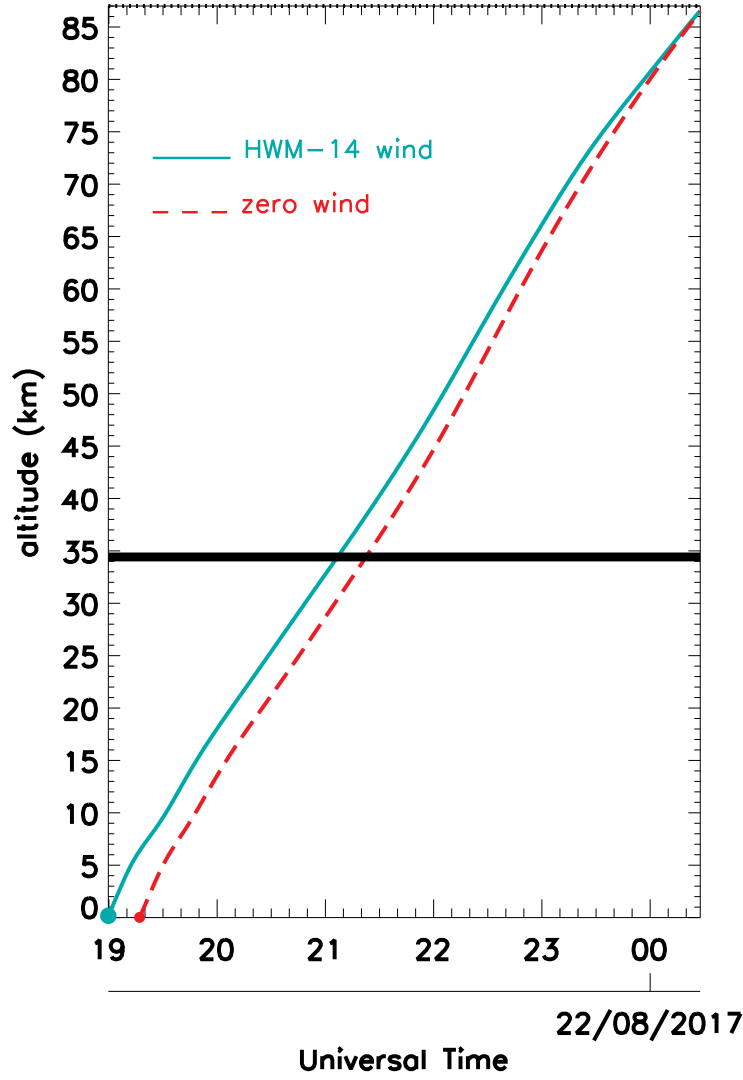


Figure 3. Extension of Figure 1 for the vertical propagation of the medium-scale AGW against the time. The horizontal black line represents the altitude where the ray path of the waves crossed the Moon's shadow.

3 Discussion

It was shown in Figure 1 that the medium-scale AGW started to be observed around 00:00 UT (21:00 local time) over São João do Cariri. This starting time is more three hours after the end of the eclipse over the Atlantic ocean. Using the horizontal phase speed of ~ 176 m/s derived from keograms, one can estimate that the wave travelled $\sim 2,218$ km in 3.5 hours. The point in which the ray path of medium-scale AGW crossed the Moon's shadow (see Figure 2) is located at 10.98°N and 28.63°W and it is $\sim 2,230$ km away from the observatory. Therefore, the propagation speed suggests that the source of the observed AGW could be at this point. Besides the Moon's shadow, there is indication of convection around that region. Moreover, around the point in which the ray-path reached the troposphere there is no indication of convection, which makes tropospheric source to be considered unlikely.

The next point to be analyzed is the vertical propagation of the medium-scale AGW derived from the reverse ray-tracing analysis. Figure 3 shows the vertical ray path of the medium-scale AGW inferred using HWM-14 winds and no winds for comparison purposes. The ray paths for the two cases are similar since the AGW had a high horizontal phase speed and it could easily escape from critical and turning levels in the atmosphere. Figure 3 shows that the wave would have travelled for more than five hours from the surface up to the OH layer and it would have crossed the Moon's shadow at around 34.4 km altitude and 21:06 UT (wind model condition). From this point onwards, it took more than 3 hours for the wave to reach the OH layer altitude of ~ 87 km. Therefore, according to the ray-tracing results, potential source for the observed AGW would be located in the stratosphere (~ 34 km altitude) over 11°N and 28.5°W .

In general, deep convection clouds, like the ones that can be seen in Figure 2 near the end of the path of the eclipse extend up to a pressure level of about 70 hPa, which is approximately 17.7 km in altitude (e.g., Sherwood et al., 2004). So, one can wonder if such a structure could excite gravity waves in the stratosphere. Observations during the Spread-F experiment (SpreadFEx) campaign carried out also over Brazil in 2005 found similar convective plumes (Vadas et al., 2009). Vadas and Fritts (2009) calculated the effects of a single convective plume and small convective cluster that can be compared to the present case study. They found that the most dominant spectrum of AGWs generated by these plumes included small-scale gravity waves with a horizontal wavelength shorter than 400 km and reaching the OH layer altitudes within an hour. Therefore, the only possible way that the observed convective system could excite gravity waves in the stratosphere would be through body forcing producing secondary gravity waves in the stratosphere, which is unlikely according to the simulations made by Vadas and Fritts (2009).

Given the lack of plausible convection sources, the eclipse become a strong candidate as the source of AGWs along the path of the Moon's shadow by the screening of the ozone layer from solar heating. Predictions of AGWs generated by eclipse showed dominant periodicities in the atmospheric fields from 2 to 4 hours (Fritts & Luo, 1993). This is in good agreement with the present observations. They have, however, calculated the horizontal scale of the structures more likely to be observed in the lower thermosphere to be over 5,000 km.

Optical observations by Aushev et al. (2008) also revealed periodicities associated with the 29 March 2006 total solar eclipse in good agreement with the present results. Furthermore, a wide spectrum of TIDs has been observed during eclipses with periods ranging from a few minutes (e.g., Davis & Da Rosa, 1970) up to a couple of hours (e.g., J. Y. Liu et al., 1998), which is close to the period of the observed medium-scale AGW.

Regarding the 21 August 2012 total solar eclipse, a temperature reduction of 1 K and increase by a factor of 2 in the ozone were predicted by Whole Atmosphere Community Climate Model-eXtended (McInerney et al., 2018). As a result of these changes in the atmospheric composition and dynamics, large-scale disturbances (TIDs) were observed in the ionosphere associated with the eclipse (e.g., Coster et al., 2017). Finally, a wave-like signature of the bow wave generated by the eclipse was observed in the neutral winds by a Fabry-Perot interferometer over São João do Cariri (Harding et al., 2018) and over Carbondale (37.7°N , 89.2°W) using airglow red and green lines (Aryal et al., 2019).

4 Conclusions

In summary, a medium-scale AGW was detected associated with the 21 August 2017 eclipse. Of particular importance is that the wave was observed at low latitudes and about 2,000 km away from the eclipse path (umbra). The AGW was observed using an all-sky imager located in São João do Cariri approximately 3 hours after the end of the eclipse. The wave had an observed period of ~ 2.5 hours and an horizontal wavelength of $\sim 1,620$ km. Additionally, the observations showed that the wave propagated to the southwest with an azimuth of $\sim 200^\circ$ clockwise from the North.

The spectral characteristics of the observed wave match theoretical prediction for AGW generated by solar eclipses. Furthermore, reverse ray-tracing simulations were performed and the results corroborate with potential wave sources located around 11°N , 28.5°W and 34 km altitude, which was the position where the gravity wave ray path crossed the Moon's shadow in the stratosphere. This is the first time that a gravity wave generated by an eclipse was captured by an all-sky airglow camera in the MLT region during the nighttime.

Acknowledgments

Airglow images from São João do Cariri can be accessed online in the portal of the "Estudo e Monitoramento Brasileiro do Clima Espacial" (EMBRACE/INPE) at <http://www2.inpe.br/climaespacial/portal/en>. Ray-tracing simulations can be accessed on <https://is.gd/paulino>. The cloud top brightness temperature maps were provided by the Center for Weather Forecasting and Climate Studies (CPTEC/INPE) at <http://satelite.cptec.inpe.br/acervo/goes16.formulario.logic>. I. Paulino, C. M. Wrasse, A. R. Paulino, E. R. de Paula, C. M. Denardini, I. S. Batista and D. Barros thank to the Conselho Nacional de Desenvolvimento Científico e Tecnológico (CNPq) for the support under contracts 303511/2017-6, 307653/2017-0, 460624/2014-8, 202531/2019-0, 303643/2017-0, 306844/2019-2 and 300974/2020-5. A. R. Paulino thanks to the Coordenação de Aperfeiçoamento de Pessoal de Nível Superior (CAPES) for the scholarship. F. S. Rodrigues would like to thank support from NSF (Award AGS-1554926). C.A.O.B. Figueiredo thanks to the Fundação de Amparo à Pesquisa do Estado de São Paulo (FAPESP) for kindly providing financial support through the process number 2018/09066-8.

Authors' contribution: IP wrote the manuscript and did most of the airglow analysis. CAOBF performed the spectral analysis of the gravity waves and revised the manuscript. FSR revised the manuscript and interpretation. RAB contributed to running the experiments in São João do Cariri during the eclipse and revised the manuscript. CMW helped with the analysis and interpretation and revised the manuscript. ARP helped with the interpretation of the results and revised the manuscript. DB provided the database for the ray-tracing. HT, ISB, AFM, PPB, MAA, ERP, CMD, LML, RYCC and JJM supported the coordinated multi-instrumented observations during the eclipse and revised the manuscript.

Competing interest: The authors declare that they have no conflict of interest.

References

- Afraimovich, E. L., Voeykov, S. V., Perevalova, N. P., Vodyannikov, V. V., Gordienko, G. I., Litvinov, Y. G., & Yakovets, A. F. (2007). Ionospheric effects of the march 29, 2006, solar eclipse over kazakhstan. *Geomagnetism and Aeronomy*, 47(4), 461–469. doi: 10.1134/S0016793207040068
- Altadill, D., Solé, J. G., & Apostolov, E. M. (2001). Vertical structure of a gravity

- 338 wave like oscillation in the ionosphere generated by the solar eclipse of august
339 11, 1999. *Journal of Geophysical Research: Space Physics*, 106(A10), 21419–
340 21428. doi: 10.1029/2001JA900069
- 341 Amabayo, E., Anguma, S., & Jurua, E. (2014). Research article tracking the iono-
342 spheric response to the solar eclipse of november 03, 2013. *International Jour-
343 nal of Atmospheric Sciences*, 2014. doi: 10.1155/2014/127859
- 344 Anderson, R. C., & Keefer, D. R. (1975). Observation of the temperature and
345 pressure changes during the 30 june 1973 solar eclipse. *Journal of the Atmo-
346 spheric Sciences*, 32(1), 228–231. doi: 10.1175/1520-0469(1975)032<0228:
347 OOTAP>2.0.CO;2
- 348 Aplin, K., & Harrison, R. (2003). Meteorological effects of the eclipse of 11 august
349 1999 in cloudy and clear conditions. *Proceedings of the Royal Society of Lon-
350 don. Series A: Mathematical, Physical and Engineering Sciences*, 459(2030),
351 353–371. doi: 10.1098/rspa.2002.1042
- 352 Arendt, P. (1972). Ionospheric undulations during the solar eclipse of 7 march 1970.
353 *Journal of Atmospheric and Terrestrial Physics*, 34(4), 719 - 725. doi: https://
354 doi.org/10.1016/0021-9169(72)90159-6
- 355 Aryal, S., Geddes, G., Finn, S. C., Mrak, S., Galkin, I., Cnossen, I., ... Chakrabarti,
356 S. (2019, 2020/05/13). Multispectral and multi-instrument observation of
357 tids following the total solar eclipse of 21 august 2017. *Journal of Geophysical
358 Research: Space Physics*, 124(5), 3761–3774. doi: 10.1029/2018JA026333
- 359 Aushev, V. M., Lyahov, V. V., López-González, M. J., Shepherd, M. G., & Dryn,
360 E. A. (2008). Solar eclipse of the 29 march 2006: Results of the optical mea-
361 surements by morti over almaty (43.03 °n, 76.58 °e). *Journal of Atmospheric
362 and Solar-Terrestrial Physics*, 70(7), 1088–1101. doi: https://doi.org/10.1016/
363 j.jastp.2008.01.018
- 364 Batista, I. S., Candido, C. M. N., Souza, J. R., Abdu, M. A., de Araujo, R. C., Re-
365 sende, L. C. A., & Santos, A. M. (2017). F3 layer development during quiet
366 and disturbed periods as observed at conjugate locations in brazil: The role of
367 the meridional wind. *Journal of Geophysical Research: Space Physics*, 122(2),
368 2361–2373. doi: 10.1002/2016JA023724
- 369 Beer, T., Goodwin, G. L., & Hobson, G. J. (1976). Atmospheric gravity wave pro-
370 duction for the solar eclipse of october 23, 1976. *Nature*, 264(5585), 420–421.
371 doi: 10.1038/264420a0
- 372 Beer, T., & May, A. N. (1972). Atmospheric gravity waves to be expected from
373 the solar eclipse of june 30, 1973. *Nature*, 240(5375), 30–32. doi: 10.1038/
374 240030a0
- 375 Broche, P., & Crochet, M. (1975). Generation of atmospheric gravity waves by the
376 30 june 1973 solar eclipse in africa. *Journal of Atmospheric and Terrestrial
377 Physics*, 37(10), 1371 - 1374. doi: https://doi.org/10.1016/0021-9169(75)90130
378 -0
- 379 Campos, J., Paulino, I., Wrasse, C., Medeiros, A. F., Paulino, A. R., & Buriti,
380 R. A. (2016). Observations of small-scale gravity waves in the equatorial
381 upper mesosphere. *Brazilian Journal of Geophysics*, 34(4), 469–477. doi:
382 10.22564/rbgf.v34i4.876
- 383 Chen, G., Zhao, Z., Zhang, Y., Yang, G., Zhou, C., Huang, S., ... Sun, H. (2011).
384 Gravity waves and spread es observed during the solar eclipse of 22 july 2009.
385 *Journal of Geophysical Research: Space Physics*, 116(A9). doi: 10.1029/
386 2011JA016720
- 387 Chimonas, G. (1974). Internal gravity-wave motions induced in the earth’s atmo-
388 sphere by a solar eclipse. In *The upper atmosphere in motion* (p. 708–714).
389 American Geophysical Union (AGU). doi: 10.1029/GM018p0708
- 390 Chimonas, G., & Hines, C. O. (1970). Atmospheric gravity waves induced by a solar
391 eclipse. *Journal of Geophysical Research (1896-1977)*, 75(4), 875–875. doi:
392 10.1029/JA075i004p00875

- 393 Chimonas, G., & Hines, C. O. (1971). Atmospheric gravity waves induced by a solar
394 eclipse, 2. *Journal of Geophysical Research (1896-1977)*, 76(28), 7003–7005.
395 doi: 10.1029/JA076i028p07003
- 396 Clemesha, B., & Batista, P. (2008). Gravity waves and wind-shear in the {MLT} at
397 23 °s. *Advances in Space Research*, 41(9), 1472 - 1477. doi: 10.1016/j.asr.2007
398 .03.085
- 399 Coster, A. J., Goncharenko, L., Zhang, S.-R., Erickson, P. J., Rideout, W., & Vier-
400 inen, J. (2017). Gns observations of ionospheric variations during the 21
401 august 2017 solar eclipse. *Geophysical Research Letters*, 44(24), 12,041–12,048.
402 doi: 10.1002/2017GL075774
- 403 Dare-Idowu, O., Paulino, I., Figueiredo, C. A. O. B., Medeiros, A. F., Buriti, R. A.,
404 Paulino, A. R., & Wrasse, C. M. (2020). Investigation of sources of gravity
405 waves observed in the brazilian equatorial region on 8 april 2005. *Annales Geo-
406 physicae*, 38(2), 507–516. doi: 10.5194/angeo-38-507-2020
- 407 Davis, M. J., & Da Rosa, A. V. (1970). Possible detection of atmospheric gravity
408 waves generated by the solar eclipse. *Nature*, 226(5251), 1123–1123. doi: 10
409 .1038/2261123a0
- 410 Denardini, C. M., Chen, S. S., Resende, L. C. A., Moro, J., Bilibio, A. V., Fagundes,
411 P. R., ... Bertolotto, T. O. (2018). The embrace magnetometer network for
412 south america: Network description and its qualification. *Radio Science*, 53(3),
413 288–302. doi: 10.1002/2017RS006477
- 414 Drob, D. P., Emmert, J. T., Meriwether, J. W., Makela, J. J., Doornbos, E., Conde,
415 M., ... Klenzing, J. H. (2015). An update to the horizontal wind model
416 (hwm): The quiet time thermosphere. *Earth and Space Science*, 2(7), 301–319.
417 doi: 10.1002/2014EA000089
- 418 Essien, P., Paulino, I., Wrasse, C. M., Campos, J. A. V., Paulino, A. R., Medeiros,
419 A. F., ... Lins, A. N. (2018). Seasonal characteristics of small- and medium-
420 scale gravity waves in the mesosphere and lower thermosphere over the brazil-
421 ian equatorial region. *Annales Geophysicae*, 36(3), 899–914. doi: 10.5194/
422 angeo-36-899-2018
- 423 Figueiredo, C. A. O. B., Takahashi, H., Wrasse, C. M., Otsuka, Y., Shiokawa, K., &
424 Barros, D. (2018). Medium-scale traveling ionospheric disturbances observed
425 by detrended total electron content maps over brazil. *Journal of Geophysical
426 Research: Space Physics*, 123(3), 2215–2227. doi: 10.1002/2017JA025021
- 427 Fritts, D. C., & Luo, Z. (1993). Gravity wave forcing in the middle atmosphere
428 due to reduced ozone heating during a solar eclipse. *Journal of Geophysical
429 Research: Atmospheres*, 98(D2), 3011–3021. doi: 10.1029/92JD02391
- 430 Frost, A. D., & Clark, R. R. (1973). Predicted acoustic gravity wave enhancement
431 during the solar eclipse of june 30, 1973. *Journal of Geophysical Research
432 (1896-1977)*, 78(19), 3995–3997. doi: 10.1029/JA078i019p03995
- 433 Garcia, F. J., Taylor, M. J., & Kelley, M. C. (1997, Oct). Two-dimensional spectral
434 analysis of mesospheric airglow image data. *Appl. Opt.*, 36(29), 7374–7385.
435 doi: 10.1364/AO.36.007374
- 436 Hanuise, C., Broche, P., & Ogubazghi, G. (1982). Hf doppler observations of grav-
437 ity waves during the 16 february 1980 solar eclipse. *Journal of Atmospheric
438 and Terrestrial Physics*, 44(11), 963–966. doi: https://doi.org/10.1016/
439 0021-9169(82)90060-5
- 440 Harding, B. J., Drob, D. P., Buriti, R. A., & Makela, J. J. (2018). Nightside detec-
441 tion of a large-scale thermospheric wave generated by a solar eclipse. *Geophysi-
442 cal Research Letters*, 45(8), 3366–3373. doi: 10.1002/2018GL077015
- 443 Jones, B. W., & Bogart, R. S. (1975). Eclipse induced atmospheric gravity waves.
444 *Journal of Atmospheric and Terrestrial Physics*, 37(9), 1223–1226. doi:
445 https://doi.org/10.1016/0021-9169(75)90194-4
- 446 Jones, T. B., Wright, D. M., Milner, J., Yeoman, T. K., Reid, T., Chapman, P. J., &
447 Senior, A. (2004). The detection of atmospheric waves produced by the total

- solar eclipse of 11 august 1999. *Journal of Atmospheric and Solar-Terrestrial Physics*, 66(5), 363–374. doi: <https://doi.org/10.1016/j.jastp.2004.01.029>
- Knížová, P. K., & Mošná, Z. (2011, 11). Acoustic-gravity waves in the ionosphere during solar eclipse events. In M. G. Beghi (Ed.), (chap. 14). IntechOpen. doi: 10.5772/19722
- Kumar, K. V., Maurya, A. K., Kumar, S., & Singh, R. (2016). 22 july 2009 total solar eclipse induced gravity waves in ionosphere as inferred from gps observations over eia. *Advances in Space Research*, 58(9), 1755–1762. doi: <https://doi.org/10.1016/j.asr.2016.07.019>
- Kumar, S., Kumar, A., Maurya, A. K., & Singh, R. (2016). Changes in the d region associated with three recent solar eclipses in the south pacific region. *Journal of Geophysical Research: Space Physics*, 121(6), 5930–5943. doi: 10.1002/2016JA022695
- Lerfald, G., Jurgens, R., Vesecky, J., & Washburn, T. (1972). Traveling ionospheric disturbances observed near the time of the solar eclipse of 7 march 1970. *Journal of Atmospheric and Terrestrial Physics*, 34(4), 733 - 741. doi: [https://doi.org/10.1016/0021-9169\(72\)90161-4](https://doi.org/10.1016/0021-9169(72)90161-4)
- Liu, J. Y., Hsiao, C. C., Tsai, L. C., Liu, C. H., Kuo, F. S., Lue, H. Y., & Huang, C. M. (1998). Vertical phase and group velocities of internal gravity waves derived from ionograms during the solareclipse of 24 october 1995. *Journal of Atmospheric and Solar-Terrestrial Physics*, 60(17), 1679–1686. doi: 10.1016/S1364-6826(98)00103-5
- Liu, X., Xu, J., Yue, J., Vadas, S. L., & Becker, E. (2019). Orographic primary and secondary gravity waves in the middle atmosphere from 16-year saber observations. *Geophysical Research Letters*, 46(8), 4512–4522. doi: 10.1029/2019GL082256
- Makela, J. J., Meriwether, J. W., Lima, J. P., Miller, E. S., & Armstrong, S. J. (2009). The remote equatorial nighttime observatory of ionospheric regions project and the international heliospherical year. *Earth, Moon, and Planets*, 104(1), 211–226. doi: 10.1007/s11038-008-9289-0
- McInerney, J. M., Marsh, D. R., Liu, H.-L., Solomon, S. C., Conley, A. J., & Drob, D. P. (2018). Simulation of the 21 august 2017 solar eclipse using the whole atmosphere community climate model-extended. *Geophysical Research Letters*, 45(9), 3793–3800. doi: 10.1029/2018GL077723
- Mohanakumar, K., & Sankaranarayanan, D. (1982, 01). Solar eclipse of february 16, 1980 - it's effect on meteorological parameters. *Proceedings of the Indian National Science Academy*, 48A, 209.
- Narcisi, R., Bailey, A., Federico, G., & Wlodyka, L. (1983). Positive and negative ion composition measurements in the d- and e-regions during the 26 february 1979 solar eclipse. *Journal of Atmospheric and Terrestrial Physics*, 45(7), 461–478. doi: [https://doi.org/10.1016/S0021-9169\(83\)81107-6](https://doi.org/10.1016/S0021-9169(83)81107-6)
- Paul, A., Das, T., Ray, S., Das, A., Bhowmick, D., & DasGupta, A. (2011). Response of the equatorial ionosphere to the total solar eclipse of 22 july 2009 and annular eclipse of 15 january 2010 as observed from a network of stations situated in the indian longitude sector. *Annales Geophysicae*, 29(10), 1955–1965. doi: 10.5194/angeo-29-1955-2011
- Paulino, A. R., Batista, P. P., & Clemesha, R. (2012). Lunar tides in the mesosphere and lower thermosphere over cachoeira paulista (22.7°s; 45.0°w). *Journal of Atmospheric and Solar-Terrestrial Physics*, 78-79, 31–36. doi: <https://doi.org/10.1016/j.jastp.2011.04.018>
- Paulino, I., Lima, L., Marcos Denardini, C., Buriti, R., Paulino, A. R., Batista, P., ... De Paula, E. (2018, July). Observations of gravity waves in the airglow during the night of 21 August 2017 solar total eclipse over Brazil. In *42nd cospar scientific assembly* (Vol. 42, p. C1.1-30-18).
- Paulino, I., Medeiros, A. F., Vadas, S. L., Wrasse, C. M., Takahashi, H., Buriti,

- R. A., ... Gobbi, D. (2016). Periodic waves in the lower thermosphere observed by 630 nm airglow images. *Annales Geophysicae*, 34(2), 293–301. doi: 10.5194/angeo-34-293-2016
- Paulino, I., Takahashi, H., Medeiros, A. F., Wrasse, C. M., Buriti, R. A., Sobral, J. H. A., & Gobbi, D. (2011). Mesospheric gravity waves and ionospheric plasma bubbles observed during the copex campaign. *Journal of Atmospheric and Solar-Terrestrial Physics*, 73(11), 1575–1580. doi: <https://doi.org/10.1016/j.jastp.2010.12.004>
- Picone, J. M., Hedin, A. E., Drob, D. P., & Aikin, A. C. (2002). Nrlmsise-00 empirical model of the atmosphere: Statistical comparisons and scientific issues. *Journal of Geophysical Research: Space Physics*, 107(A12), SIA 15–1–SIA 15–16. doi: 10.1029/2002JA009430
- Rodrigues, F. S., Shume, E. B., de Paula, E. R., & Milla, M. (2013). Equatorial 150 km echoes and daytime f region vertical plasma drifts in the brazilian longitude sector. *Annales Geophysicae*, 31(10), 1867–1876. doi: 10.5194/angeo-31-1867-2013
- Schödel, J. P., Klostermeyer, J., & Röttger, J. (1973). Atmospheric gravity wave observations after the solar eclipse of june 30, 1973. *Nature*, 245(5420), 87–88. doi: 10.1038/245087a0
- Sears, R. (1972). Ionospheric hf doppler dispersion during the eclipse of 7 march 1970 and tid analysis. *Journal of Atmospheric and Terrestrial Physics*, 34(4), 727–732. doi: [https://doi.org/10.1016/0021-9169\(72\)90160-2](https://doi.org/10.1016/0021-9169(72)90160-2)
- Sherwood, S. C., Minnis, P., & McGill, M. (2004). Deep convective cloud-top heights and their thermodynamic control during crystal-face. *Journal of Geophysical Research: Atmospheres*, 109(D20). doi: 10.1029/2004JD004811
- Shiokawa, K., Otsuka, Y., & Ogawa, T. (2009). Propagation characteristics of nighttime mesospheric and thermospheric waves observed by optical mesosphere thermosphere imagers at middle and low latitudes. *Earth, Planets and Space*, 61(4), 479–491. doi: 10.1186/BF03353165
- Sivakandan, M., Paulino, I., Ramkumar, T. K., Taori, A., Patra, A. K., Sripathi, S., ... Bilibio, A. V. (2019). Multi-instrument investigation of troposphere-ionosphere coupling and the role of gravity waves in the formation of equatorial plasma bubble. *Journal of Atmospheric and Solar-Terrestrial Physics*, 189, 65–79. doi: <https://doi.org/10.1016/j.jastp.2019.04.006>
- Sivakandan, M., Paulino, I., Taori, A., & Niranjana, K. (2016). Mesospheric gravity wave characteristics and identification of their sources around spring equinox over indian low latitudes. *Atmospheric Measurement Techniques*, 9(1), 93–102. doi: 10.5194/amt-9-93-2016
- Vadas, S. L., & Fritts, D. C. (2009). Reconstruction of the gravity wave field from convective plumes via ray tracing. *Annales Geophysicae*, 27(1), 147–177. doi: 10.5194/angeo-27-147-2009
- Vadas, S. L., Taylor, M. J., Pautet, P.-D., Stamus, P. A., Fritts, D. C., Liu, H.-L., ... Takahashi, H. (2009). Convection: the likely source of the medium-scale gravity waves observed in the oh airglow layer near brasilia, brazil, during the spreadex campaign. *Annales Geophysicae*, 27(1), 231–259. Retrieved from <http://www.ann-geophys.net/27/231/2009/> doi: 10.5194/angeo-27-231-2009
- Vargas, F. (2019). Gravity wave activity over the andes lidar observatory (alo) generated by the july 2, 2019 full solar eclipse observed in chile. *Earth and Space Science Open Archive*, 1. doi: 10.1002/essoar.10501368.1
- Zerefos, C. S., Gerasopoulos, E., Tsagouri, I., Psiloglou, B. E., Belehaki, A., Herekakis, T., ... Mihalopoulos, N. (2007). Evidence of gravity waves into the atmosphere during the march 2006 total solar eclipse. *Atmospheric Chemistry and Physics*, 7(18), 4943–4951. doi: 10.5194/acp-7-4943-2007